A Semi-Autonomous Terminal Phase Spacecraft Docking Attitude Determination and Control System Simulator

Cengiz B. Akinli

Dr. Christopher D. Hall, Advisor
Department of Aerospace and Ocean Engineering
Virginia Polytechnic Institute and State University
Interim Report

December 18, 2003
Blacksburg, Virginia

1. Introduction

In 1965, after being catapulted into only the second manned orbital spaceflight of the Gemini program, Gemini 4, pilot Jim McDivitt made an attempt to catch up to his spent upper stage booster, and in so doing, became the very first person to attempt spacecraft rendezvous with another body. Unfortunately, the results of his attempt were not promising. When he pointed his capsule at his target and fired his rear thrusters, he effectively moved away from the target. Since this maneuver was far from a primary mission objective, it received the forethought mission managers apparently felt it deserved: very little. It didn't take flight engineers long at all to figure out what went wrong. They had failed to account for the obvious effects of orbital motion in their maneuver. In simple terms when McDivitt pointed his spacecraft at the target out in front of him and fired his thrusters, he increased his orbital energy, which translates into a higher orbit and a lower angular velocity around the earth. So his target began to outrun him just like a slower runner can outrun a faster one by being on the inside lane of a track.

Spacecraft docking has come a long way since then, and is today almost exclusively fully automated. One of the primary reasons for this is the counterintuitive effects of the non-inertial orbital reference frame on relative motion, as demonstrated by Gemini 4. But even without that factor, subsequent experimentation has shown that humans have an exceedingly difficult time judging relative distances and velocities without any of the visual cues present when doing so from a car, boat, or aircraft. Thus, manual docking quickly developed into a fly-by-the-gauge practice, which is exactly the type of maneuver that is best suited for automation.

Autonomous Rendezvous and Capture (ARC) can be thought of as three distinct phases. First, coarsely computed, pre-planned orbital maneuvers are executed to bring the maneuvering spacecraft, called the chase spacecraft, within close proximity, generally 100 meters, of the target body with or without continuous feedback from low resolution, long range sensors, generally radar, detecting relative position. Second, the final 100 meters is closed using continuous feedback from high precision, short range sensors, generally optical in nature, reporting the relative attitude and position of the chase spacecraft from the target. Finally, upon contact, some type of grappling mechanism is deployed to physically connect the two bodies (hard dock).

This research focuses entirely on the final 100 meters of closure, often referred to as the terminal phase of rendezvous, with a strong, albeit not exclusive, focus on the determination and simple control of the attitude of the chase spacecraft. It should be noted that although a reference frame fixed on the target body in any orbit around another central body is not inertial, we assume that it is, and that this assumption is a common and acceptable one to make, given that the 100 meter range and the relatively short time over which the maneuver is simulated make the effects of orbital motion relatively minute.

Using a spacecraft simulation platform based on a hemispherical air bearing, giving us 3 degree-of-freedom motion (360º rotation about the vertical axis and ±10º rotation about the other two), we develop an attitude determination and control system based on a distributed, optical attitude sensor and a cold gas thruster based control system.

Attitude determination is realized by a laser and sensor system based on a set of four nearly parallel laser beams in an rhomboid pattern emitted from the chase spacecraft and detected by a sensor grid on the target. The relative positions of the points of incidence of the beams to one another allows for the computation of all relative position data. Since the beams are not perfectly parallel, but each slightly inclined toward the geometric center of the rhomboid, the size of the projected ellipse is used to compute range data. Since the lasers are arranged in an rhomboid, the orientation about the sensor normal axis is straightforward to determine. Likewise, the eccentricity and major axis orientation of the ellipse defined by the four points of incidence is used to calculate angle between the range vector and sensor normal axis (the φ angle in spherical coordinates centered on the sensor grid) and the angle between the range vector and x axis (the θ angle in spherical coordinates) respectively.

An important consideration in docking operations is the change in sensor precision with respect to range. Generally, maximum precision is required at the minimum range, just prior to hard dock. Inclination of the laser beams toward, rather than away from the center imposes a maximum operating range, but also provides for increasing precision with decreasing range, as the relative size of the projected triangle increases as the range decreases. Additionally, if the inclination angle is such that the beams converge to a point within the specified maximum range, then diverge again, operational range is limited only by the size of the target on which the target points will fit after diverging. This leaves a blind spot when the range is reduced to that of beam convergence, but is a potentially worthwhile configuration that will be explored in future research.

Attitude control is provided by a cold gas thruster system incorporating six thrusters and a single automatic pressure regulator, providing throttle control. In the initial phase of operation, the thruster system is under manual control to effect coarse orientation of the chase so that the targeting lasers are visible on the target sensor. Once this is achieved, the autonomous system assumes control of the chase and the simulates the rest of the docking maneuver.

2. Literature Review

Of central focus to this research is the terminal phase of spacecraft docking, conventionally defined as the final 100 meters of approach, wherein a number of assumptions may be made, including that of an inertial frame of reference fixed on the target spacecraft, ignoring the effects of orbital motion on maneuvers, and that of the absence of any perturbing moments and forces which, though small, would otherwise be worth examining considering the relatively high precision required for the maneuver we are attempting. Yet, such considerations are beyond the scope of this research and will be ignored.

We now review a number of existing absolute and relative attitude sensor systems discussed in existing literature. A well-developed system is the Video Guidance Sensor (VGS) under development at the Marshall Space Flight Center (MSFC) of the National Aeronautics and Space Administration (NASA). Under development since 1987, the VGS, and now its successor, the Advanced Video Guidance Sensor (AVGS) have undergone a series of refinements and now constitute a highly robust and reliable system capable of delivering highly precise relative attitude and position data for ranges between .5 m and 200 m.

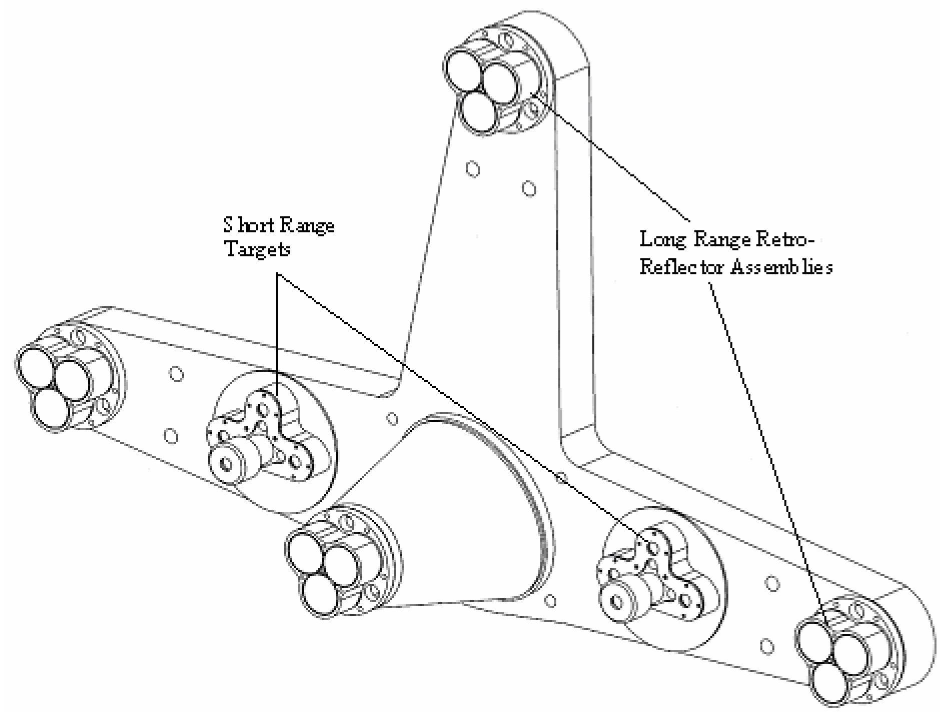

Figure 1 - The Video Guidance Sensor

The AVGS is a video-based sensor consisting of an active sensor head and a passive target. The optical target consists of one long range and two short range sets of retroreflectors. The long range set consists of four sets of three corner cube retroreflectors mounted on the target spacecraft in a T configuration, with the three outermost sets in a single plane and the central set elevated from that plane along the docking axis. The spacing between the central retroreflector set and each of the peripheral retroreflector sets is approximately 44 cm, and the central set is elevated approximately 20 cm along the docking axis. The short range targets each consist of four individual cornercube retroreflectors arranged in the same pattern as the long range target but on a much smaller scale. These targets are mounted in between the central and the two collinear retroreflector sets of the long range targets.

Each retroreflector is covered by a filtering lens that passes light around 850 nm and absorbs light near 800 nm. The target is illuminated twice in a short time span, first at 850 nm then, .033 seconds later, at 800 nm wavelength. The 850 nm light passes through the filters and returns to the camera as well as reflecting incidentally from other surfaces within the target area. The 800 nm light is absorbed by the filters but still reflects incidentally from the other surfaces within the target area. The second image is then digitally subtracted from the first, effectively filtering out returns from ambient light and other reflective surfaces. The result is a very low noise image which, once a proper threshold is applied, contains only the target spots.

The VGS sensor head consists of an analog CCD camera surrounded by eight laser diodes, four emitting light at each of the wavelengths, placed as close as possible to the edge of the camera lens. This is necessary because the use of cornercube retroreflectors means that light is returned from them directly to the source. Thus the camera must be situated within the coverage area of the reflected beams. One issue arising from this with the VGS is that at close range, the coverage area of the reflected beams is sufficiently small so as not to encompass the camera lens. This is the primary limiting factor from which the minimum operational range of the sensor is derived, and though the short range targets are covered with plano-concave lenses to increase the beam divergence, the effect is still only somewhat mitigated. This has been addressed in the design of the AVGS by incorporating a 45° angled mirror in front of the lens, allowing the laser flight path and the boresight of the camera to be truly coaxial.\\

Another key improvement in the AVGS is the use of a digital complementary metal oxide semiconductor (CMOS) camera rather than a conventional analog charge coupled device (CCD) and digital frame grabber. The CCD limits the capture rate to the 30 fps of standard analog video, which imposes an arbitrary upper limit on the scan rate of the sensor. Additionally, using the frame grabber allows for delivery of only complete frames of video imagery rather than just that portion of the field of view that is of interest (i.e. where the target is know to be located). The CMOS camera is a fully digital image sensor which can be subsampled for faster, coarser scans, or windowed so that only the area immediately surrounding the target is scanned. Also, the CMOS camera can essentially be sampled at whatever rate the controlling computer is capable of sampling, placing no upper limit on the sensor's effective scan rate.\\

Other types of sensors offer different advantages, however. A scanning telegoniometer will be used on the Automatic Transfer Vehicle (ATV) of the European Space Agency (ESA) and the Japanese H-II Transfer Vehicle (HTV). Unlike the fixed lasers of the VGS and AVGS, a telegoniometer laser scans the sensor's entire FOV, detecting relative bearing and range of retroreflectors comprising the target. The scan is effected by two moving mirrors, one for horizontal and one for vertical scanning. The bearing to each retroreflector is determined by the mirror positions which are in turn determined by standard optical encoders on the mirror shafts. The range to each reflector is determined by calculating the flight time of the laser. The primary advantage of this system is that video sensing, and the coupled computationally intensive task of determining 3 dimensional position from a 2 dimensional image data are both unnecessary.\\

A primary disadvantage of a scanning telegoniometer is that the use of reciprocating mirrors can be a source of substantial perturbations in a maneuver like docking, which requires the highest possible precision. Unlike the VGS systems, which have no moving parts, the telegoniometer depends on mirrors which rotate across the FOV and reverse, causing vibrations within the system. Another disadvantage is the potential for noise. The VGS and AVGS dual wavelength illumination scheme is among the most sophisticated video imaging attitude determination schemes currently in use. The signal to noise ratio of these sensors are an order of magnitude higher than any other. A scanning telegoniometer illuminates its target once, with a single wavelength of light, and must depend merely on simple thresholding to distinguish target retroreflectors from other reflective surfaces or ambient light sources within the FOV.

3. System Operation

3.1.1 Assumptions

A number of assumptions are made within the scope of this research and should be disclosed prior to a description of the system and its operation. We assume firstly that the body fixed frame of the target spacecraft is inertial, meaning both that the target is non-rotating and not accelerating. The latter is substantial, especially in low Earth orbit, where any spacecraft is accelerating substantially. Still this assumption is a reasonable approximation if the time of the maneuver is small and the distance separating the target and chase spacecraft is short. This is a very common assumption made in far more advanced treatments of spacecraft rendezvous and docking and is made explicitly for the purpose of disposing of the complexities of orbital motion, which are outside the scope of this research.

3.1.2 Definitions

For clarity, a number of terms are defined here, along with the axis system used throughout this paper. The chase and target spacecraft refer to the controlled spacecraft and non-moving, uncontrolled spacecraft respectively. Rendezvous refers to closure of two spacecraft to a distance of 100 meters a zero closure velocity.

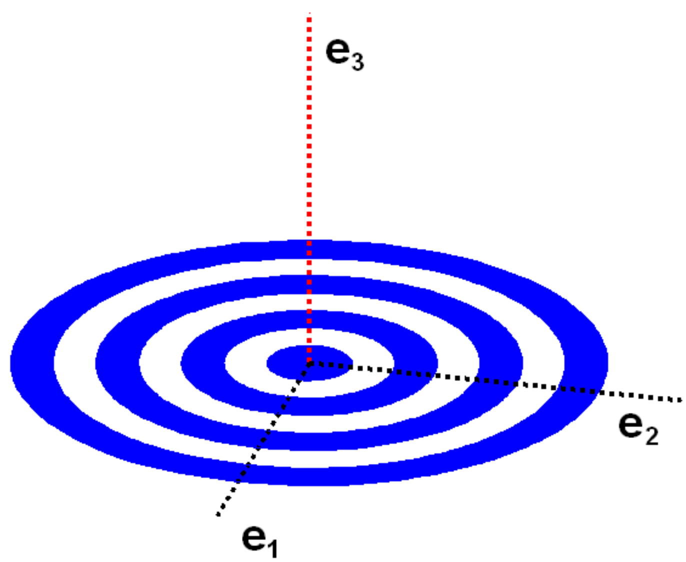

Figure 2 - Axis system

Fig. 2 shows the axis system referred to throughout this paper. The bulls eye target is the surface of the target spacecraft upon which the docking operation will occur. The e_3 axis is referred to as the "docking axis," along which the chase spacecraft will approach the target.

3.2 System Description

The docking sensor system consists of two parts, a laser emitter array mounted on the chase spacecraft, and a sensor grid mounted on the target spacecraft. The system controls the attitude of the chase spacecraft, which is simulated by an air bearing spacecraft simulator, using a set of six cold gas thrusters, which provide simultaneous control of roll, pitch, and yaw.

The laser emitter array is a set of four laser emitters that emit beams in nearly the same direction, but slightly inclined toward a common axis, about which the emitters themselves are placed equidistantly. The inclination angle may be such that either the point of convergence of the beams is just beyond the specified maximum range of operation of the system, or the point of convergence is within that range, allowing the beams to diverge at ranges beyond the point of convergence. Such a configuration could more than double the range over which the system is operable with the only effect being that relative roll and position data of the chase would be indeterminable exactly at that range, effectively producing a blind spot for the system.

The sensor grid is a translucent deflector mounted on the target in front of a camera capable of detecting multiple wavelengths of scattered laser light by effectively seeing the laser points on an otherwise uniformly colored deflector. The camera image is read digitally by on computer onboard the target and relayed to the chase computer.

The thruster system is a set of three pairs of opposed cold gas thrusters, each of which consists of a gas solenoid valve and subsonic converging nozzle connected to a common automatic electronically controlled gas pressure regulator. The regulator provides a means of controlling the maximum pressure provided to the entire set of thrusters, giving throttle control over the system. The pairs of thrusters are arranged so as to provide full three axis control of the chase spacecraft simulator simultaneously. The target spacecraft is stationary in this simulation.

3.3 Operation

The system operates in two distinct modes:

1. Manual target acquisition
2. Automatic alignment, ranging, and closure

Phase 1 is effected by direct manual control of the thruster system through a remotely manipulated manual input device. The current implementation uses a gaming joystick connected to an offboard computer. That computer relays the input device position to the computer onboard the chase spacecraft. Each axis of the joystick provides control input for direct, linear control of one pair of thrusters. Associating the yaw, pitch, and roll axes of the joystick with the corresponding thruster pairs onboard the chase simulator allows for highly intuitive control of the chase attitude via the human interface.

Further, the electronic regulator allows for real time control of the pressure supplied to the thruster system. Thus, rather than using the input device position to determine simple on/off states for each of the six thrusters, the precise position of each input device axis can set effective throttle values for the corresponding thruster pack, ranging smoothly from -100% to 100% on each axis.

While the entire system is supplied by a single automatic regulator, all three axes may be independently throttled by pulsing one or more thrusters. If a single thruster is active, meaning two of the axes are commanded to be at 0% throttle, then the regulator is simply set to the appropriate pressure for that single axis

$$X \rightarrow P = \frac{X}{P_{\max}} \tag{1}$$

Here X is the commanded throttle setting between 0 and 1. P is the pressure control signal sent to the regulator, and P_{max} is the value of P corresponding to the maximum possible pressure.

If however, two or three axes are active at once, the thrusters on the additional axes may pulse at a fixed frequency with a duty cycle computed to effect their respective commanded throttle settings, while the regulator is set to provide the pressure corresponding to the highest throttle setting of all three axes. The duty cycles of the thrusters for the axes with lesser commanded thrust are determined by

$$Y \rightarrow D_Y = \frac{Y}{X} \tag{2a}$$

$$Z \rightarrow D_Z = \frac{Z}{X} \tag{2b}$$

Here, Y and Z are the two lesser commanded throttle settings regardless of the axes to which they correspond. The axis with the highest commanded throttle setting at any instant is designated as the X axis for control purposes. It should be noted that these designations are unrelated to common spatial coordinate axis designations.

Ideally, this arrangement would provide for fully independent throttle control over all three axes. However, experimentation has proven that the electronic regulator is not capable of sufficiently fast reactions to additional valve openings so as to keep the effect of pressure fluctuations on the already open thrusters negligibly small. Thus, opening a second thruster valve while one is already open affects the thrust of that first thruster significantly. Thus, the control of regulator pressure includes hooks to compensate for the pulsing of additional thrusters such that Eq. (1) is modified to

$$P = f\left(\frac{X}{P_{\max}}, Y, Z\right) \tag{3}$$

where the function f accounts for the throttle settings of the lesser axes as well and increases the regulator setting accordingly. The exact function f has not been determined as experimentation to characterize multiple thruster operation is currently ongoing.

Phase 2 is initiated by an operator signal, before which the sensor system is completely passive, processing no input data at all. Upon activation, the system executes a number of tests to determine if the system is within a controllable state. The questions these tests are meant to answer are:

1. Can the chase relative attitude be determined given the current state? (Are all the laser spots on the target?)
2. Are the chase yaw and pitch rates nullable? (Or will the laser spots leave the target before the system can stop any existing motion?)

If the answer to both questions is effectively yes, the system assumes control. The four points visible to the sensor allow for the calculation of a unique ellipse. The first action of the control system is to align the chase relative roll angle. The roll angle is determined by the angular offset of a line from the geometric center of the ellipse to a designed laser point.

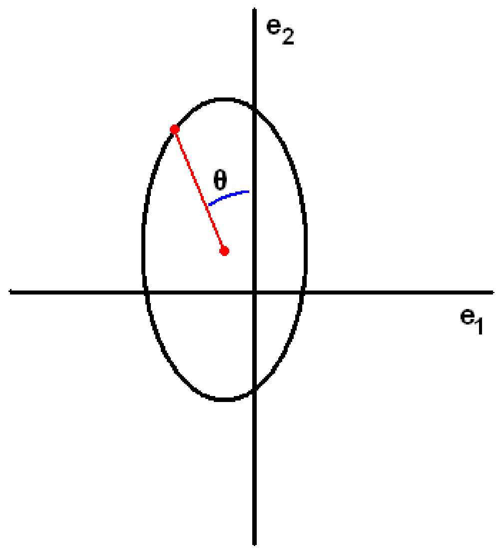

Figure 3 - Chase spacecraft relative roll angle

The roll angle is illustrated in Fig. 3, which also shows the geometric center of the ellipse, which is not specifically illuminated by a laser, but rather calculated once the ellipse is calculated. The system then aligns the pitch and yaw angles of the chase so that that geometric center aligns with the center of the e_1-e_2 plane.

Position offset, the displacement of the chase spacecraft from the docking axis, is related to the eccentricity of the ellipse. If the ellipse is perfectly circular, then the chase is on the docking axis. If the ellipse is highly eccentric, then the chase is displaced from the docking axis, looking at the target at a steep angle. Furthermore, the orientation of the semi-major axis of the ellipse may be used to calculate the orientation of that displacement.

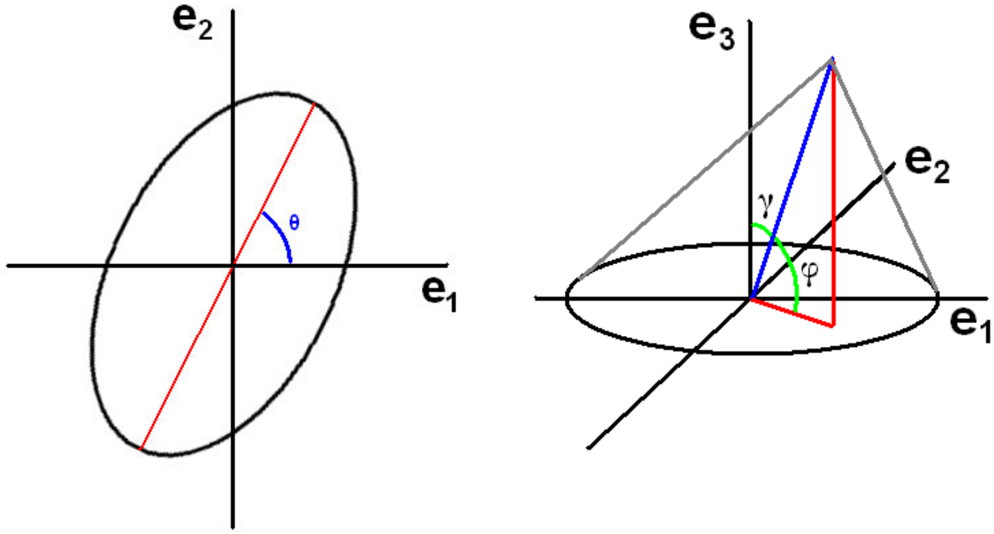

(a) semi-major axis length and orientation (b) eccentricity determines φ

Figure 4 - Eccentricity and semi-major axis show position offset

If we express the position of the chase relative to the target using spherical coordinates, then we see from Fig. 4 that r is related to the semi-major axis of the ellipse, θ is related to the angle between the semi-major and e_1 axes, and φ is related to the eccentricity of the ellipse.

4. Specific Issues

4.1 Relative Precision of Chase and Target Attitude Measurements

4.1.1 Chase Attitude

The precision of the chase spacecraft relative attitude measurement is an order of magnitude greater than that of its position. Firstly, we note that the position measurement can be illustrated as a relative attitude measurement of the target with respect to the chase, as any orbit of the chase about the target can be simulated by a simple rotation of the target. Hence, the problem may be approached as an attitude/position problem or as an attitude/attitude problem. The following is an analysis based on the latter using a target configuration similar to the Video Guidance Sensor (VGS) developed at the Marshall Space Flight Center. While we limit ourselves to a two dimensional analysis for illustrative purposes here, it is easily seen that the assertions made here may be fairly extrapolated to three dimensions.

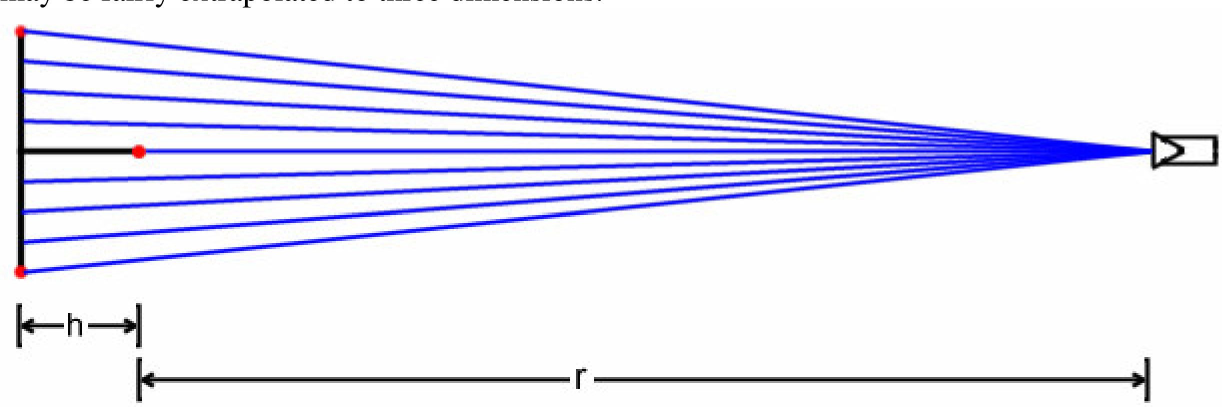

Figure 4

This target is a planar arrangement of three target spots as shown in Figure 1. The center spot is a distance r from the camera. The outer spots are approximately a distance $h + r$ from the camera, assuming r is much greater than h and that the angular separation of the three spots in the camera's field of view is small. In the position shown in Fig. 4, the three spots appear as three collinear dots in the center of the camera's field of view (FOV). The pixel centers of the image generated by the camera are illustrated. At the given distance, the separation of the three dots represent a total spread of eight pixels in the image generated by the camera.

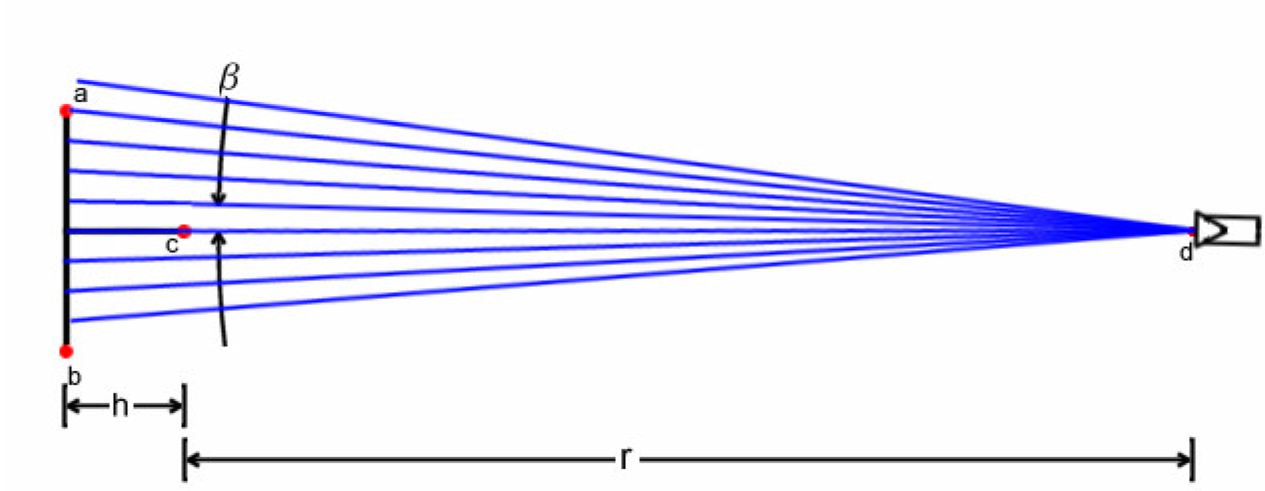

Figure 5

It is immediately obvious that the minimum detectable rotation of the chase is merely that which causes point c to move a minimum of one pixel in the camera image, which is the angle β, which in turn, is approximately the camera's field of view divided by the image pixel size near the center of the field of view. Hence, the precision of the chase relative attitude measurement is independent of range (as long as the range is sufficiently small such that the spots are detectable and distinguishable).

4.1.2 Target Attitude

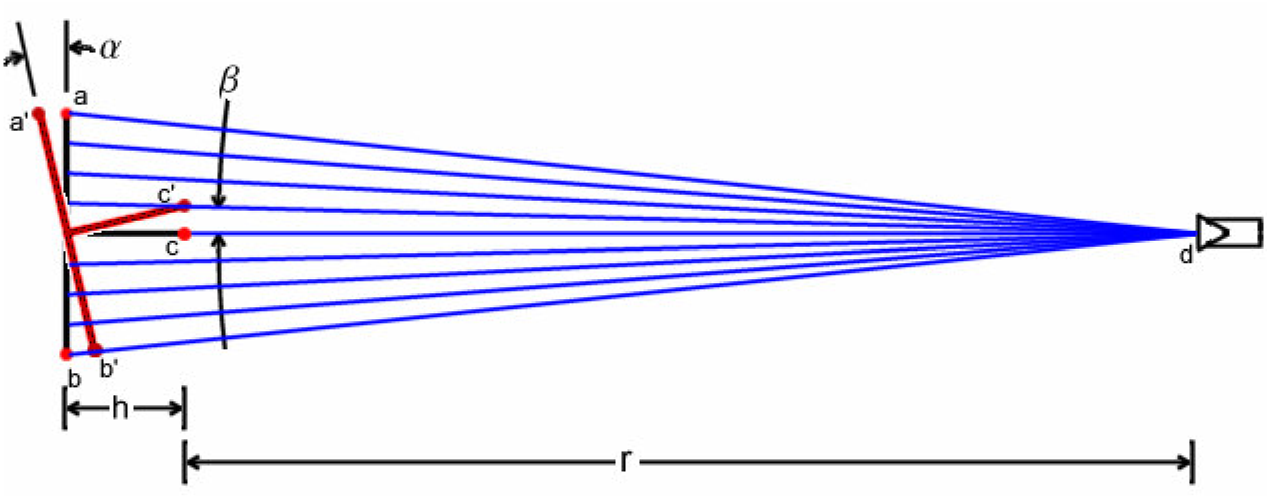

Figure 6

However, the precision of the target relative attitude measurement is range dependent. As with rotation of the chase, there is a minimum detectable target rotation, α.

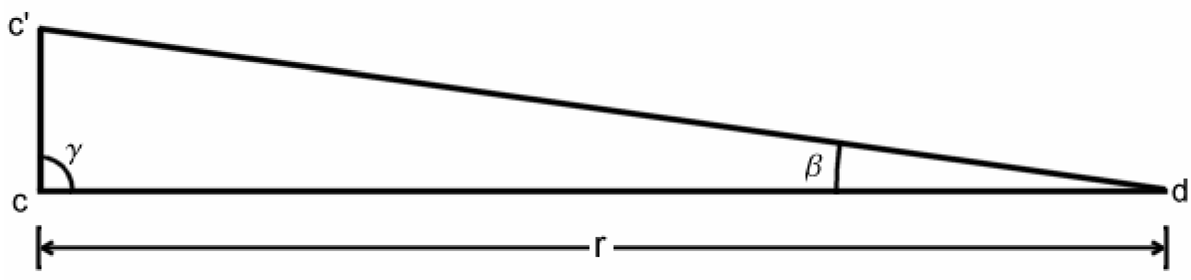

Figure 5

We assume that the target rotation angle α is small. As a result, we may conclude that c' is almost directly above c and γ is approximately 90º. As before, β is the angular pixel separation in the camera generated image. From Fig. 6, we see that $cc'=h\sin\alpha$. From Figure 4, we see that $cc'=r\sin\beta$. Equating the two gives:

$$\frac{\sin\alpha}{\sin\beta}=\frac{r}{h}$$

If we assume that r is larger than h, which is true down to the minimum operating range of the VGS, then it easily seen that α is larger than β. Thus, the minimum detectable rotation of the target is larger than the minimum detectable rotation of the chase.

4.2 Camera Placement

For the guidance sensor previously proposed, placement of the visual sensor on the target addresses range dependent deterioration of the precision of the chase relative attitude measurement.

We note that placement of the camera is a primary factor in the overall system configuration. Placement on the chase spacecraft results in a system where the components on the chase illuminate reflective points on the target, and the video system measures the relative position of those points with respect to the center point in its FOV. Placement on the target results in a system of one or more lasers to actively create the targeting spots on a reflective or translucent optical target.

. Aboard the chase, a video camera would be able to detect a chase rotation of the same fixed angle β as in the previous discussion. Chase rotation would result in movement of the target spot(s) across the camera FOV. The minimum detectable rotation would be that which results in a movement of at least one pixel. However, aboard the target, the same camera can detect a chase rotation angle that actually decreases with increasing range.

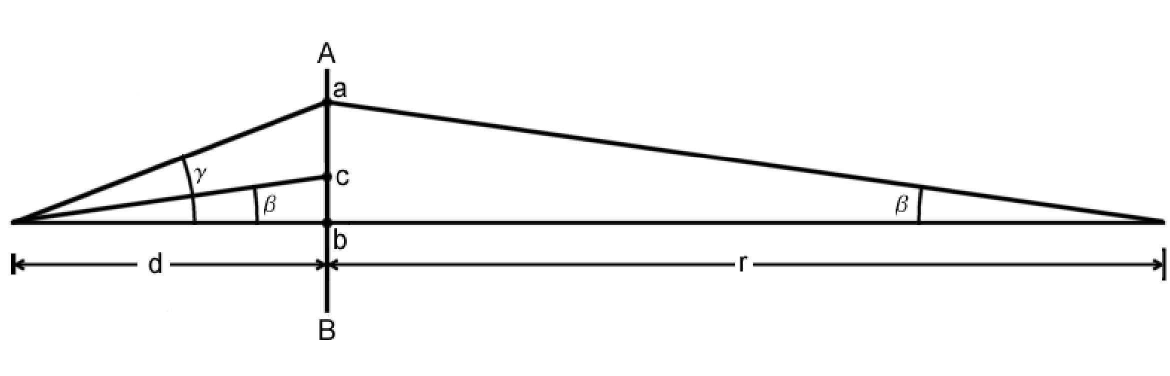

Figure 6

Points *a* and *b* are the target points after and before rotation of the chase through an angle β. With the camera aboard the target, the resulting motion of the target spot represents an angular separation in the camera FOV of γ, which is larger than β. Specifically, $\tan\beta = ab/r$ and $\tan\gamma = ab/d$. Combining these equations yields

$$\frac{\tan\gamma}{\tan\beta} = \frac{r}{d}$$

Assuming both angles are small, we see

$$\frac{\gamma}{\beta} = \frac{r}{d}$$

Since *r* will always be larger than *d*, we see that a rotation of β produces an angular pixel separation γ that is far larger than the minimum measurable angular separation of the camera if the camera is aboard the target.

5. Conclusion

This paper presented a review of some of the most current literature covering the topic of relative attitude determination for ARC operations, highlighting the issues most pertinent to the level of research involved in this project, presented a proposed solution using available air bearing spacecraft simulators and other readily available hardware, and addressed the most pressing issues currently being faced in this ongoing project. Specific issues raised during the research were discussed and solutions to the more major dilemmas were detailed.

The overall problem addressed in this research is not novel, but rather well-traveled, with highly developed solutions already in use. It is not the goal of this researcher to merely mimic those existing solutions nor to abandon the principles employed and discoveries made by their creators entirely, but rather to use the best of the knowledge gained in the development of those solutions to create a limited solution which may be fully implemented in this limited laboratory environment.

References

[1] Erwin, H.O. Laser Docking System, AAS 84-033, pages 239-253

[2] Howard, R.T. et al. An Advanced Sensor for Automated Docking, delivered by author

[3] Howard, R.T. et al. Active Sensor System for Automatic Rendezvous and Docking, delivered by author

[4] Howard, R.T. et al. Video Guidance Sensor Flight Experiment Results, delivered by author

[5] Jackson, John L. et al. Automatic Docking System Sensor Analysis & Mission Performance, delivered by author

[6] Jackson, John L. et al. Video Guidance Sensor - Optical Performance Predictions and Results from STS-95 Flight Experiment, delivered by author

[7] Howard, R.T. et al. The Video Guidance Sensor: Space, Air, Ground, and Sea, delivered by author

[8] Howard, R.T. et al. The Video Guidance Sensor - A Flight Proven Technology, AAS 99-025, delivered by author

[9] Howard, R.T. et al. Video-based sensor for tracking 3-dimensional targets, NASA technical report #4167-43, delivered by author

[10] Strietzel, Roland. Selected Aspects of Attitude Sensors for Spacecrafts. *Space Technology*, 21(4):163-181

[11] Strietzel, Roland. Precise Attitude Determination for Rendez-vous and Docking by Information Fusion of Laser Range Finder Measurements, IAC-02-A.3.06

[12] Moebius, Bettina and Kolk, Karl-Hermann. RendezVous Sensor for Automatic Guidance of Transfer Vehicle to ISS - Concept of the Operational Modes Depending on Actual Optical and Geometrical Dynamical Conditions. In *Proceedings of the Photonics for Space Environments VII Conference*, San Diego, California, 31 July-1 August 2000. The International Society for Optical Engineering.

[13] Kolk, Karl-Hermann and Moebius, Bettina. Rendez-Vous sensor for automatic guidance of transfer vehicles to the International Space Station. In *Proceedings of the Photonics for Space Environments VII Conference*, San Diego, California, 31 July-1 August 2000. The International Society for Optical Engineering.

[14] Ho, Chi-Chang J. and McClamroch, N. Harris. Automatic Spacecraft Docking Using Computer Vision-Based Guidance and Control Techniques. *Journal of Guidance, Control, and Dynamics,* 16(2):281-288, March-April 1993.